Michael Stritt*, Tobias Oesterlein, Stefan Pollnow, Armin Luik, Claus Schmitt and Olaf Dössel

Assessment of local high-density mapping for the analysis of radiofrequency ablation lesions in the left atrium

Abstract: Recent studies about the development of endocardial radiofrequency (RF) ablation lesions (ALs) tried to identify reliable electrogram (EGM) markers for assessment of lesion transmurality. Additional clinically relevant information for physicians can be provided by examining endocardial EGM parameters like signal morphology, amplitude or time points in the signal. We investigated EGM features of the pulmonary vein ostia before and after RF ablation for three point-shaped lesions. Using high-density (HD) mapping, local activation time (LAT) and voltage maps were created, which provided information about the RF ALs regarding the lesion size and showed activation time delay as well as low-voltage areas with bipolar peak-to-peak voltages smaller than 2 mV. The time delay of the depolarization front comparing the activation times anterior and posterior to the RF AL was up to 51.5 ms. In a circular area with 5 mm radius around an RF AL the mean peak-to-peak voltage decreased by 62-94 % to about 0.12-0.44 mV and the mean maximal absolute EGM derivative was reduced by 65-96 %. Comparing the results of this study with EGMs of similar clinical settings confirmed our expectations regarding the low-voltage areas caused by the ablation procedure. An improved understanding of the electrophysiological changes is of fundamental importance to provide more information for enhanced RF ablation assessment.

Keywords: High-Density Mapping, Radiofrequency Ablation, Left Atrium, Point-Shaped Lesions, Intracardiac Electrograms.

https://doi.org/10.1515/cdbme-2017-0176

***Corresponding author: Michael Stritt:** Institute of Biomedical Engineering, Karlsruhe Institute of Technology (KIT), Kaiserstr. 12, 76128 Karlsruhe, Germany, e-mail: publications@ibt.kit.edu
Tobias Oesterlein, Stefan Pollnow, Olaf Dössel: Institute of Biomedical Engineering, Karlsruhe Institute of Technology (KIT), Kaiserstr. 12, 76128 Karlsruhe, Germany, e-mail: publications@ibt.kit.edu
Armin Luik, Claus Schmitt: Städtisches Klinikum Karlsruhe, Moltkestraße 90, 76133 Karlsruhe, Germany, e-mail: kardiologie@klinikum-karlsruhe.de

1 Introduction

Cardiac arrhythmias like atrial fibrillation or atrial flutter are commonly treated with radiofrequency (RF) ablation [1, 2]. However, recurrence of these tachycardias is a widespread medical problem. To check the ablation lesion (AL) formation and the total success of a Pulmonary Vein Isolation (PVI), previous studies focused on examining transmurality using different electrogram (EGM) criteria of uni- and bipolar EGMs. It was possible to differentiate between the formation of transmural and non-transmural lesions using uni- and bipolar EGM criteria [3]. Further studies also determined that the reconnection occurrence after PVI decreased and the sinus rhythm maintenance rate was improved when taking EGM criteria into account [4]. Therefore, formation of point-shaped lesions can be indirectly assessed using EGM criteria [1, 3, 4]. The research focus of our study was to examine the electrophysiological changes before and after ablation using different cardiac mapping techniques in combination with a modern high-density (HD) mapping system. The results of a previous study from Keller [1] on a similar clinical setting will be compared for the task of finding reliable parameters for the AL identification and the overall lesion evaluation. To conclude, we validated the results by comparing the AL characteristics and the common voltage ranges with a definition from a previous animal study from Thajudeen [5].

2 Methods

2.1 Data acquisition

Data were recorded during a routine clinical catheter ablation at *Städtisches Klinikum Karlsruhe* with written informed consent. During catheter ablation, three point-shaped RF ALs were created using a 4 mm irrigated IntellaNav OI ablation catheter from Boston Scientific. The RF ALs were located in the left atrial ostia on a line for PVI. The position of each AL was tagged during the procedure, shown as white dots in figure 1.

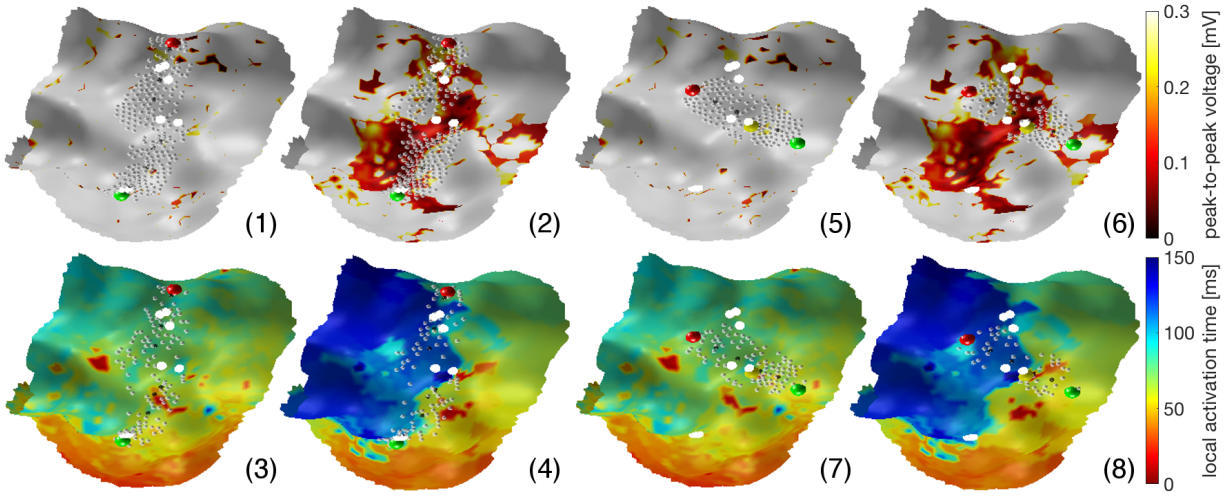

Figure 1: Path-Driven Electrograms (PDEGMs) are used to analyze the data points of LAT or voltage maps along a straight line along the endocardial surface. Vertical PDEGMs: (1-4). Horizontal PDEGMs: (5-8). (1) & (5) voltage maps before ablation, (2) & (6) voltage maps after ablation, (3) & (7) LAT maps before ablation, (4) & (8) LAT maps after ablation. Voltage maps (1), (2), (5) and (6) rely on NSR data. LAT maps (3), (4), (7) and (8) rely on PE data. Posterior view of the left atrium. Green and red dot: start and end position, yellow dot: position close to the RF AL, white dots: RF AL tags, small grey dots: data points.

Before and after ablation, mapping was conducted using Rhythmia, a modern HD electroanatomical mapping system. The acquired data sets included 12 body surface electrocardiogram (ECG) channels as well as EGMs from the Orion mini-basket mapping catheter and an 8 electrode Coronary Sinus (CS) catheter. All catheters were produced by Boston Scientific (USA). In order to reduce signal noise and baseline wander this study focuses on bipolar signals. For that reason the 64 Orion electrodes from 8 different splines were combined to 56 bipolar signals. The CS catheter electrodes one to six were used to determine three bipolar signals, since electrode 7 was used for pacing. In the clinical setup a sensed pacing protocol was applied that emitted a pacing impulse after three normal sinus rhythm (NSR) events. For the further analysis we therefore differentiated between NSR and paced excitations (PEs).

2.2 EGM analysis: ECG, CS and Orion

Before the detection of intracardiac activities the data sets were preprocessed. Body surface ECGs were filtered with a Butterworth bandpass filter from 0.3-30 Hz. The EGMs of the CS and the Orion were filtered with a 1-300 Hz Butterworth bandpass and multiple Notch filters. Fiducial Points (FPs) of the ECG signals were determined using institution internal algorithms of Gustavo Lenis [6]. To analyze the EGMs of the CS, the ventricular far-field (VFF) was blanked with a piecewise cubic spline interpolation and the current R peak time points from the FP algorithm. The time range for this interpolation was chosen after visual inspection. Atrial activities (AAs) were detected using the Non-Linear Energy Operator (NLEO) from Schilling et al. [2] with thresholds depending on the standard deviation of the corresponding NLEO signal. Pacing in CS electrode 7 was identified using a fixed threshold depending on the maximal negative derivative of the EGM. For the differentiation between NSR events and PEs we used the R peaks detected with the FP algorithm in combination with the detected pacing events.

For the analysis of the Orion EGMs, the VFF was blanked the same way as in the CS data processing. To structure the 56 bipolar signals, the AAs of the CS were chosen as the reference for the AAs in the intracardiac EGMs of the Orion catheter. For each AA detected in the CS a window of 150 ms for NSR excitations and 200 ms for PEs was cut out of the Orion signals. The 56 bipolar Orion signal windows of each AA detected in the CS were then labeled as NSR or PE. EGMs recorded further away than 5 mm from the endocardial triangulated surface mesh (TSM) were excluded from further analysis. After calculating the peak-to-peak (P2P) values of the AAs in the Orion signal windows, the NLEO was applied to compute the local activation time (LAT) relative to the CS AA in the signal windows. To detect AAs with the NLEO we used a threshold depending on the standard deviation of the signal. AAs with a relative low P2P value raised doubts as to whether these AAs are only signal interferences or noise. Therefore these AAs were eliminated using a fixed threshold defined as the 0.15-quantile of all AA P2P values. In the data post-processing we rechecked the LAT samples and excluded AAs by applying a P2P quantile as a threshold for the P2P value within a small range anterior and posterior to the LAT

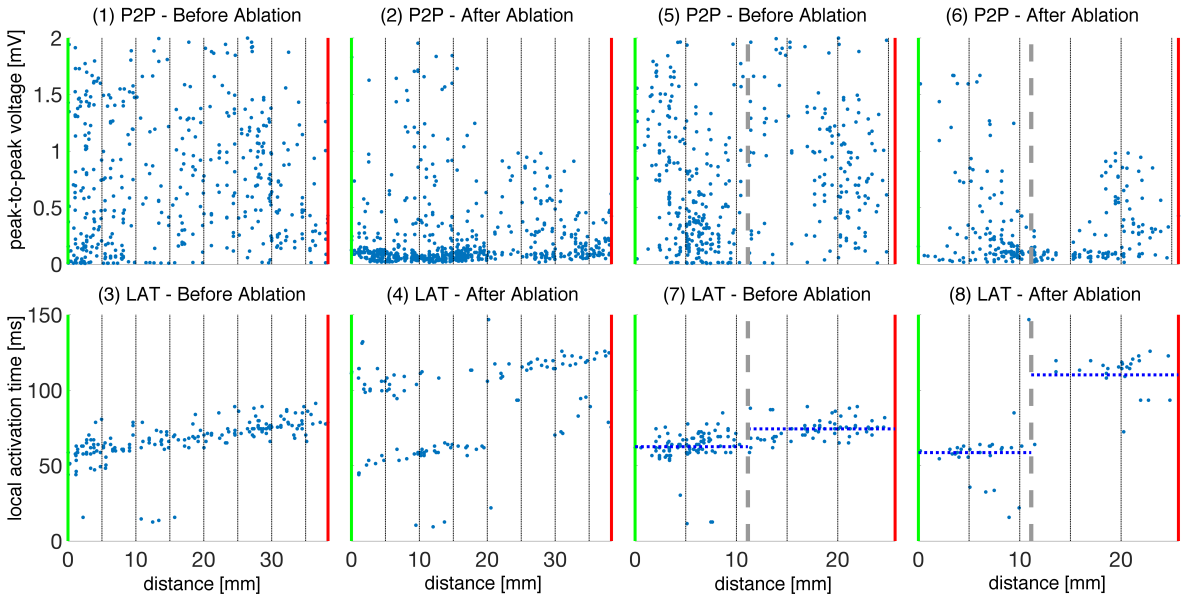

Figure 2: Signal statistics for the Path-Driven EGMs (PDEGMs). Vertical PDEGMs: (1-4). Horizontal PDEGMs: (5-8). Blue points: P2P or LAT values of the small grey dots shown in figure 1, green line: start position, corresponding to the green dot, gray line: position close to the RF AL, corresponding to the yellow dot, red line: end position, corresponding to the red dot in figure 1.

Table 1: Relative changes of bipolar electrograms in a circular area with 5 mm radius around each radiofrequency ablation lesion: Mean peak-to-peak (P2P) voltage and mean maximal absolute EGM derivative (MAD).

	ablation lesion 1	ablation lesion 2	ablation lesion 3
P2P	**-61.9 %**	**-80.3 %**	**-93.8 %**
MAD	**-65.3 %**	**-87.3 %**	**-96.2 %**

sample. This was done to eliminate AAs where a P2P value was found to be caused by baseline wander or signal interferences, which themselves arose from sources of electromagnetic disturbances or damaged tissue.

2.3 Map interpolation and generation

We projected the data on the electroanatomical TSM and interpolated areas by using the Nearest Neighbor algorithm. In the event that multiple data points were projected on an individual TSM vertice, we calculated the mean value. The additional data were kept to perform the statistical analysis, as can be seen in figure 2, where all AAs of every measurement in range are depicted. The projected data was either the LAT or the P2P value, resulting in LAT and voltage maps as shown in figure 1. Statistical comparison of values before and after ablation was performed in a circle of 5 mm radius around each ablation lesion.

2.4 Generating the path-driven EGMs

We implemented an algorithm to investigate the LAT and voltage data along a straight line on the endocardial surface. First, a start and an end point are chosen that are colored in green and red. It is then possible to choose a point close to the RF AL, which is colored in yellow. The Path-Driven EGM (PDEGM) algorithm searches for every data point along the path. The distance to the start point is then used as a measure for the total distance and drawn along the x-axis. The y-axis can be used for the LAT or the P2P value. We evaluated horizontal paths (orthogonal to the ablation line) and vertical paths (parallel to the ablation line) across all ALs (shown in figure 1).

3 Results

Figure 1 shows the LAT and voltage maps before and after ablation. Also visualized are the measurement points taken into account for the vertical and horizontal PDEGMs along a straight line. The maps of the PDEGMs before ablation, maps (1), (3), (5) and (7) of figure 1, have neither a delay of the LAT nor low-voltage areas. After ablation the voltage maps (2) and (6) of figure 1 have clearly visible low-voltage areas around the RF AL tags. The PDEGM LAT maps after ablation, maps (4) and (8), have a distinct delay of the LAT comparing the areas anterior and posterior to the RF AL tags. The signal

statistics of these PDEGMs can be seen in figure 2. Before ablation, the HD mapping data demonstrated a large spread of values for individual points and there is no LAT delay, represented by the wide spread of P2P values in plot (1) and (5) and the slow increase of the LAT values in plot (3) and (7) of figure 2. The LAT delay of 51.5 ms of the area posterior to the yellow dot can be seen in plot (8) of figure 2. This delay is calculated using the mean values of the data points before and after the yellow dot, which then result in the blue lines of the plots (7) and (8). Besides these results, we also calculated the changes of the mean P2P voltages and the mean maximal absolute EGM derivatives of areas with a 5 mm radius around each RF AL, displayed in table 1.

4 Discussion

Comparing the voltage maps before and after ablation, there is a clearly visible connection between AL tags and low-voltage areas. The amount of lower P2P values after ablation can be seen in plots (2) and (6) of figure 2 as well. The horizontal PDEGMs of plot (6), however, show the connection of the lower voltages in the area between 10 and 15 mm, relative to the start point, and the RF AL more intuitively. After ablation the P2P voltages decreased by 62-94 %, first row of table 1, which agrees with the expected outcome. In the clinical study of Keller [1], the relative minimum of bipolar EGMs decreased by 20 ± 33 % and the relative maximum by 95 ± 17 %. The mean P2P values after ablation of 0.12-0.44 mV match the definition of an RF AL of Thajudeen [5], who declared ALs to be areas with bipolar P2P voltages smaller than 1 mV. The mean maximal absolute EGM derivative $max(|\frac{dV}{dt}|)$, which is decreasing as well (second row of table 1), matches the clinical study of Keller [1], who measured a relative change of the maximum deflection $max(\frac{dV}{dt})$ of -79 ± 10 %. Combining the visual investigation of the voltage and LAT maps with the statistical data helps evaluating the RF AL formation, regarding lesion geometry and possibly transmurality as well. The LAT maps after ablation displayed an unexpected wide conduction block along the later PVI line of the three point-shaped RF ALs. This could be a temporal effect, caused by inflammation or edema as a result of the RF ablation heat. Measurement errors caused by the movement of the patient, the catheter, the heart or the blood flow may also influence the results. To answer the question where this conduction block or LAT delay is originating, a further clinical study with a similar scenario is required to make a statistically verified statement about the changes of LAT. The high spatial resolution of the anatomy and the additional data even in low-voltage areas with a lesser availability of evaluable EGMs are notable advantages of HD mapping. Searching for more RF AL markers and the improvement of the currently used criteria detection could definitely help to support the clinical research.

Author's Statement: Research funding: Stefan Pollnow is supported by a scholarship of the Karlsruhe School of Optics and Photonics (KSOP). This project was supported by the German Research Foundation (DFG grant DO 637/20-1). Conflict of interest: Authors state no conflict of interest. Informed consent: Informed consent has been obtained from all individuals included in this study. Ethical approval: The research related to human use complies with all the relevant national regulations, institutional policies and was performed in accordance with the tenets of the Helsinki Declaration, and has been approved by the authors' institutional review board or equivalent committee.

References

[1] Keller MW, Schuler S, Wilhelms M et al. Characterization of Radiofrequency Ablation Lesion Development Based on Simulated and Measured Intracardiac Electrograms. IEEE Trans Biomed Eng 2014; 61: 2467–2478.

[2] C. Schilling, M. Nguyen, A. Luik, et al. Non-Linear Energy Operator for the Analysis of intracardial Electrograms. World Congress on Medical Physics and Biomedical Engineering. Munich, Germany. Springer, 2009, 872–875.

[3] Otomo K, Uno K, Fujiwara H, Isobe M, Iesaka Y. Local unipolar and bipolar electrogram criteria for evaluating the transmurality of atrial ablation lesions at different catheter orientations relative to the endocardial surface. Heart Rhythm 2010; 7: 1291–1300.

[4] Bortone A, Appetiti A, Bouzeman A, et al. Unipolar signal modification as a guide for lesion creation during radiofrequency application in the left atrium: A prospective study in humans in the setting of paroxysmal atrial fibrillation catheter ablation. Circ Arrhythmia Electrophysiol 2013; 6: 1095–1102.

[5] A. Thajudeen, W. M. Jackman, B. Stewart, et al. Correlation of Scar in Cardiac MRI and High-Resolution Contact Mapping of Left Ventricle in a Chronic Infarct Model. Pacing and Clinical Electrophysiology, 2015, 38(6): 663–674.

[6] Gustavo Lenis, Tobias Baas and Olaf Dössel. Ectopic beats and their influence on the morphology of subsequent waves in the electrocardiogram. Biomedizinische Technik/Biomedical Engineering. Germany, 2013, 58(2): 109-119.